Received: 26 January 2023 | Revised: 29 June 2023 | Accepted: 5 July 2023

DOI: 10.1111/ele.14291

ECOLOGY LETTERS cnrs WILEY

PERSPECTIVE

Structural asymmetry in biotic interactions as a tool to understand and predict ecological persistence

Alfonso Allen-Perkins[1] | **David García-Callejas**[2,3] | **Ignasi Bartomeus**[4] | **Oscar Godoy**[5]

[1]Departamento de Ingeniería Eléctrica, Electrónica, Automática y Física Aplicada, ETSIDI, Technical University of Madrid, Madrid, Spain

[2]School of Biological Sciences, University of Canterbury, Christchurch, New Zealand

[3]Landcare Research, Lincoln, New Zealand

[4]Estación Biológica de Doñana (EBD-CSIC), Seville, Spain

[5]Departamento de Biología, Instituto Universitario de Ciencias del Mar (INMAR), Universidad de Cádiz, Puerto Real, Spain

Correspondence
Alfonso Allen-Perkins, Departamento de Ingeniería Eléctrica, Electrónica, Automática y Física Aplicada, ETSIDI, Technical University of Madrid, 28040 Madrid, Spain.
Email: alfonso.allen.perkins@gmail.com

Funding information
Ministerio de Ciencia e Innovación, Grant/Award Number: PID2021-122711NB-C21, PID2021-127607OB-I00 and RTI2018-098888-A-I00; Ministerio de Economía y Competitividad, Grant/Award Number: RYC2017-23666

Editor: Shaopeng Wang

Abstract

A universal feature of ecological systems is that species do not interact with others with the same sign and strength. Yet, the consequences of this asymmetry in biotic interactions for the short- and long-term persistence of individual species and entire communities remains unclear. Here, we develop a set of metrics to evaluate how asymmetric interactions among species translate to asymmetries in their individual vulnerability to extinction under changing environmental conditions. These metrics, which solve previous limitations of how to independently quantify the size from the shape of the so-called feasibility domain, provide rigorous advances to understand simultaneously why some species and communities present more opportunities to persist than others. We further demonstrate that our shape-related metrics are useful to predict short-term changes in species' relative abundances during 7 years in a Mediterranean grassland. Our approach is designed to be applied to any ecological system regardless of the number of species and type of interactions. With it, we show that is possible to obtain both mechanistic and predictive information on ecological persistence for individual species and entire communities, paving the way for a stronger integration of theoretical and empirical research.

KEYWORDS
asymmetry, biotic interactions, coexistence, feasibility domain, prediction, nonlinear population dynamics, persistence, structural approach

INTRODUCTION

Ecologists seek to obtain a mechanistic understanding of the processes governing the dynamics of ecological systems. The meaning of *mechanistic*, however, varies across ecological levels of organization. For instance, while biotic interactions are key for a mechanistic understanding of community dynamics (Levine et al., 2017), so is plant growth for population ecologists or photosynthesis rates for ecophysiologists (Peñuelas et al., 2011). Nevertheless, a common trade-off across fields is that obtaining such mechanistic understanding often comes at the cost of losing predictive ability (Dietze, 2017; Petchey et al., 2015; Tredennick et al., 2021). These mismatches between understanding ecological processes and predicting ecological dynamics are due to multiple causes, yet a common limitation is the lack of correspondence between the mathematical tools used for understanding and those used for predicting. For instance, in community ecology, while the mechanistic understanding of complex dynamics of interacting species uses well-established population models (Bimler et al., 2018; Godoy & Levine, 2014), predictive studies are much less developed and generally use a completely different set of tools including machine learning techniques (Civantos-Gómez et al., 2021; Evans et al., 2011).

In order to break the methodological trade-off between understanding and predicting, recent approaches have

applied tools from the structuralist approach (Saavedra et al., 2020; Song et al., 2020). In mathematics, structural stability is a property of dynamical systems that defines the range of conditions compatible with stable dynamics. Applied to ecological communities, the structuralist approach posits that the structure of species interactions influences the opportunities for multiple species to persist in the long term and, therefore, their coexistence (Godoy et al., 2018; Saavedra et al., 2017). The larger these opportunities (measured as the size of the so-called feasibility domain), the larger the range of environmental conditions the community can withstand without losing any species. Among other insights, it has been predicted (Saavedra et al., 2017), and empirically shown (Bartomeus et al., 2021; García-Callejas et al., 2023) that this situation occurs when species experience strong self-regulation and niche differentiation. These insights are probabilistic in nature (Cenci et al., 2018), coherent with the principle that is impossible to quantify the whole set of abiotic and biotic factors modulating community dynamics (Shoemaker et al., 2019).

The occurrence, sign and strength of biotic interactions are arguably the most relevant information needed to understand and predict ecological outcomes at the species and the community level (Macarthur, 1957). As such, biotic interactions are the raw material that the structuralist approach uses to define the feasibility domain, which in turn allows for predicting the persistence of whole communities (i.e. community feasibility), species composition or abundances at equilibrium (Tabi et al., 2020). For instance, it has been shown that in both random and empirical communities, the size of the feasibility domain (i.e. the range of species growth rate values compatible with persistent communities) is dependent on the type of interaction, mean interaction strength and connectance (Grilli et al., 2017). However, the distribution of interaction strengths is not only relevant to determine the size, but equally important, the shape of the feasibility domain. Conceptually speaking, if all species interact in the same way the feasibility domain will be symmetrical, but in practice, interactions among species in real-world systems are predominantly asymmetric (Adler et al., 2018; Bascompte et al., 2006). That is, species generally differ in their pairwise per-capita effects $\alpha_{ij} \neq \alpha_{ji}$. These asymmetries in interactions translate to asymmetries in the feasibility domain, as recently exemplified in communities of different types (Grilli et al., 2017) (see an additional example in Suppl. Section 1).

Understanding the asymmetry of the feasibility domain is important because it implies that not all species have the same opportunities to coexist. That is, some species are more affected than others by random changes in environmental conditions, such as interannual variations in precipitation. Therefore, even in communities with large feasibility domains, it is likely that particular species may become locally extinct when environmental conditions change. These more vulnerable species represent the 'weak spot' for the feasibility of the whole community (Grilli et al., 2017). This process was exemplified in a recent study by Tabi et al. (2020) who, working with protist communities in temperature-controlled environments, showed that in communities with more asymmetric feasibility domains, it is harder to predict which protist species went extinct first. Overall, these examples have shown that it is not only important to understand the potential of the community structure to maintain all of its constituent species, but also the relative vulnerability of each species to perturbations in their demographic performance.

Despite these recent studies providing solid and rigorous progress, it is still poorly understood how to independently quantify the shape and the size of the feasibility domain. This separation is critical to better predict ecological outcomes at the level of species and communities. Conceptually, we should aim for a shape measure that is independent of the size of the feasibility domain. Although these properties are not fully independent (see an example in Suppl. Section 2), it is currently not explored to what extent they can be meaningfully disentangled and interpreted. For instance, when measuring the shape of the feasibility domain as the heterogeneity in the distribution of the side lengths of its borders (Grilli et al., 2017), we are implicitly measuring the change in the size of the domain as well. This is because a mild increase in the variability of the side lengths of the feasibility domain implies also a change in its size. A similar conceptual problem applies to characterizing the asymmetry of the feasibility domain by computing the variability of direct effects between species pairs (Tabi et al., 2020). To advance in our ability to predict the dynamics of ecological communities, here we provide new developments that control for the correlation between the shape and size of the feasibility domain. Failing to control for this relationship may significantly hinder our ability to estimate species' vulnerabilities to exclusion in local communities.

Coupled with these methodological advances, we require empirical tests to evaluate their usefulness. Otherwise, they will remain valid theoretical constructs but with limited application to real conditions. Predictions of ecological dynamics using the structuralist approach have focused so far on either computer simulations (Grilli et al., 2017) or highly controlled laboratory (Tabi et al., 2020) and experimental settings (Bartomeus et al., 2021), yet hard tests under field conditions are scarce (Song & Saavedra, 2018). These tests are key to shed light on the applicability of the perspective we present here to predict species dynamics across a wide range of ecological systems and environmental conditions. The litmus test of ecological prediction is that of predicting species abundances (Clark et al., 2020; Tredennick et al., 2017), which is relatively uncommon due to its inherent complexity, as it encompasses a

greater degree of information than species richness or composition (McGill et al., 2007).

In this perspective, we develop and test new probabilistic metrics to understand species' relative vulnerability to exclusion from local communities, and the relationship of these metrics with temporal changes in observed abundances. In particular, we build from recent developments that quantified the minimum random perturbation that can exclude a species from a feasible community (denoted as 'full resistance' in Medeiros et al. (2021) and as 'robustness' in Lepori et al. (2023)). We propose to call this metric 'exclusion distance', which is a definition rooted in the analysis of exclusion probabilities that follows. We expand on this idea and develop a novel theory that quantifies: (1) the absolute and relative probabilities of being the first species excluded from the community (referred to as 'probability of exclusion' and 'exclusion ratio', respectively) and (2) an intuitive index that quantifies the asymmetry in species' vulnerabilities to extinction in any ecological community (referred to as the 'asymmetry index'), regardless of their overall feasibility potential. Importantly, this set of metrics can be applied to ecological communities with arbitrary interaction types and number of species. Lastly, we ask whether these metrics can inform about changes in species population growth rates through time in a grassland community composed of a diverse set of species with contrasted functional roles. We show that the metrics developed here are phenomenologically correlated with year-to-year variation in observed population growth rates across species.

THEORETICAL FRAMEWORK

Preliminaries: Definition of the feasibility domain and its size

To understand the theoretical background of this perspective, we introduce some key concepts of the structuralist approach. This framework posits that the structure of species interactions determines the opportunities for species to coexist by conditioning the size of the feasibility domain. Particular structures of species interactions, such as intraspecific competition exceeding interspecific competition, promote larger sizes of the feasibility domains and, therefore, larger opportunities for species to coexist (Barabás et al., 2016; García-Callejas et al., 2023). In order to measure the size of the feasibility domain, we need to connect the structure of species interactions with a model describing the dynamics of interacting species. The underlying model commonly used is the linear Lotka-Volterra (LV) model, as it represents a balance between tractability and complexity, and can generate population dynamics with the range of complexity of more complex models (Cenci & Saavedra, 2018; Hart et al., 2018; Saavedra et al., 2017). On the one hand, the model allows summarizing the effect of the abiotic environment on the performance (i.e. the balance between mortality and resource intake) of individual species into a single parameter, the intrinsic growth rate (Saavedra et al., 2020). On the other hand, despite its simplicity, the LV model has successfully explained and predicted the dynamics of diverse ecological systems under controlled and natural experimental conditions (García-Callejas et al., 2021; Godoy & Levine, 2014; Saavedra et al., 2020; Tabi et al., 2020; Venturelli et al., 2018). The model is of the form:

$$\frac{dN_i}{dt} = N_i\left(r_i + \sum_{j=1}^{S} \alpha_{ij} N_j\right), \quad (1)$$

where N_i denotes the abundance of species i, S is the number of species, r_i is the intrinsic growth rate of species i which represents how species i grows in isolation under given abiotic conditions, and α_{ij} is the element (i,j) of the interaction matrix $\mathbf{A}$ and represents the per-capita biotic effect of species j on the per-capita growth rate of species i.

In a given ecological community, the necessary conditions to sustain long-term positive abundances for all species depend on its interaction matrix $\mathbf{A}$, and are known as the feasibility domain of the community, henceforth FD. Formally, the FD is the parameter space of intrinsic growth rates that leads to a feasible (positive) equilibrium, that is, the set of $\mathbf{r}$ such that $\mathbf{N}^* = -\mathbf{A}^{-1}\mathbf{r} > \mathbf{0}$ for non-singular interaction matrices $\mathbf{A}$ (i.e. for matrices whose inverse, denoted as $\mathbf{A}^{-1}$, exists), where $\mathbf{r}$ is a column vector whose i-th element is the intrinsic growth rate r_i, and $\mathbf{N}^*$ is a column vector whose i-th element represents the abundance of species i when the feasible equilibrium exists, $N_i^* > 0$ (Song et al., 2018). When the points in the FD are also dynamically stable (i.e. when the real part of the eigenvalues of the linearized Jacobian matrix of Equation (1) is negative), then feasibility ensures the stable coexistence of the S species (Logofet, 2005). Despite real-world communities might no be dynamically stable, especially communities with high interaction asymmetries (Bunin, 2017), it is possible to find feasible systems with unstable equilibria. In such systems, it should be possible to evaluate at least the short-term population dynamics in response to temporal reconfigurations of the structure of biotic interactions (Medeiros et al., 2023). This is the particular case of annual communities (García-Callejas et al., 2021), which is the system we empirically test the metrics presented here.

According to the structuralist approach, the larger the size of the FD, the more likely the community can persist without any species going extinct. To quantify its size, previous work has assumed no a-priori knowledge about how the intrinsic growth rates will change within a community. For that reason, we assume that all parameter values are equally likely to be observed in the entire parameter space (Saavedra et al., 2020), and use the probability of uniformly sampling a vector of feasible

intrinsic growth rates on a representation of that space, the unit ball B^S. In mathematical terms, the probability that all species can persist, $\Omega(\mathbf{A})$, is equal to the ratio of the following volumes:

$$\Omega(\mathbf{A}) = \frac{\mathrm{vol}\left(D_F(\mathbf{A}) \cap B^S\right)}{\mathrm{vol}\left(B^S\right)}, \quad (2)$$

where $X \cap Y$ denotes the intersection of any two sets X and Y (Gourion & Seeger, 2010; Saavedra et al., 2020; Saavedra, Rohr, Fortuna, et al., 2016; Song et al., 2018). Hereafter, we denote the relative volume Ω as the size of the FD. To illustrate these mathematical expressions for a community with three species, Figure 1 shows the intersection of the FD with the unit ball. Specifically, only the points that lie within those triangles represent feasible vectors of growth rates. The vertices contained in Figure 1 (coloured circles) depict vectors of intrinsic growth rates where only a single species has positive equilibrium abundances $N_i^* > 0$ ($N_j^* = 0$ for $i \neq j$), whereas each edge shows vectors of growth rates where a given species (the species of the vertex with the same colour as the edge) goes excluded. Importantly, both communities in Figure 1 have FDs of the same size $\Omega = 0.064$ but differ in their shape. For communities with S species, the size $\Omega(\mathbf{A})$ lies between 0 and 0.5 (Song et al., 2018). Thus, the closer $\Omega(\mathbf{A})$ is to 0.5, the larger the likelihood that the structure of species interactions $\mathbf{A}$ promotes a feasible community regardless of the differences in intrinsic growth rates among species. The size $\Omega(\mathbf{A})$ presented in Equation (2) can be efficiently computed as follows:

$$\Omega(\mathbf{A}) = \frac{1}{(2\pi)^{S/2}\sqrt{|\det(\mathbf{A})|}} \int \cdots \int_{\mathbf{N}^* \geq 0} e^{-\frac{1}{2}\mathbf{N}^{*T}\mathbf{A}^T\mathbf{A}\mathbf{N}^*} d\mathbf{N}^*, \quad (3)$$

via a quasi-Monte Carlo method (Genz & Bretz, 2009; Saavedra, Rohr, Olesen, et al., 2016; Song et al., 2018).

Feasibility domain shape: Interpreting perturbations as distances

The FD's size Ω can be used as an indicator of the tolerance of a community to random environmental variations. However, two communities with the same number of species S and identical values of Ω can still have very different responses to perturbations of their intrinsic growth rates $\mathbf{r}$, depending on the shape of their FDs (Figure 1). Because this shape is critical to understand and predict the feasibility of the whole community and the vulnerability of its constituent species, we here build on a recently proposed metric (the species exclusion distance (Lepori et al., 2023; Medeiros et al., 2021)) to develop three novel metrics that thoroughly characterize such shape, namely: (1) the species' probability of exclusion, (2) their exclusion ratios and, at the community level, (3) the asymmetry index (see Box 1 for a summary of these metrics).

To introduce these metrics, we start by posing a simple question: What is the maximum perturbation in environmental conditions a community can withstand without losing species and therefore becoming unfeasible? To answer this question, first, we should consider that species go excluded when the vector of growth rates of the community $\mathbf{r}$ moves from its initial position until it reaches the border of the FD. The further away a vector of intrinsic growth rates $\mathbf{r}$ is from the border of the FD, the larger the perturbations of $\mathbf{r}$ the community can withstand while being feasible. The largest minimum distance between the growth vector $\mathbf{r}$ and the border

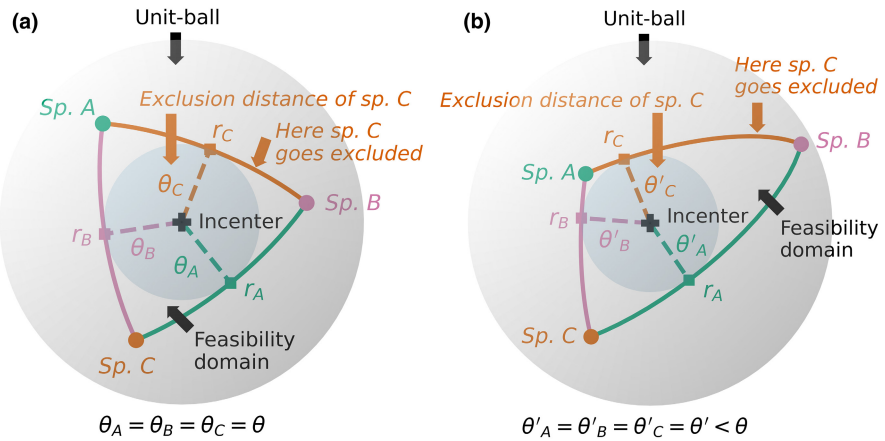

FIGURE 1 Examples of feasibility domains (FDs) for communities with $S = 3$ species. The white sphere represents the unit ball, whereas the spherical triangles show the borders of the FD. Within the spherical triangles lie the vectors of intrinsic growth rates that lead to the persistence of the three species altogether. In this example, the size of both triangles (Ω) is the same ($\Omega = 0.064$). However, in panel (a) we represent a symmetric domain (equilateral spherical triangle), whereas panel (b) shows an asymmetric one (scalene spherical triangle). The distance between the incenters of the FD (black plus markers) and their respective borders (square markers) are represented with dashed coloured lines. In addition, the blue spherical caps are a guide to the eye to compare that the minimum distance from the incenter to the edge of the FD is shorter in the asymmetric triangle. The distance between the incenter and the border is $\theta_{\text{symmetric}} = 0.417$ in panel (a), and $\theta_{\text{asymmetric}} = 0.365$ in panel (b).

BOX 1 Metrics based on the shape of the feasibility domain

Species exclusion distance. Given a feasible community whose dynamics can be well approximated with a linear Lotka-Volterra (LV) or models that can be summarized via a LV structure (Equation 1; Godoy & Levine, 2014; Saavedra et al., 2017), the exclusion distance of species i, denoted as θ_i, represents the minimum perturbation of the community's initial vector of growth rates ($\mathbf{r}_0$) that can exclude species i from that community (Lepori et al., 2023; Medeiros et al., 2021). The geometrical definitions and reasoning required for its analytical calculation (Equation S7) are presented in Suppl. Sections 3 and 4.

Probability of exclusion. This probabilistic metric, denoted as P_i^E, ranges between 0 and 1, and estimates the average (absolute) probability that species i will be the first one to be excluded if a destabilizing perturbation took place in a feasible community under LV dynamics. According to its formal definition (Equations 4 and 6), on the one hand, the calculation of these probabilities does not require an initial vector of growth rates. On the other hand, their values mainly depend on the shape of the FD. In ideal symmetric communities with S species, all species are equally likely to be the first species excluded and, consequently, the probability of exclusion of each species is given by $P_i^E = 1/S$.

Species exclusion ratio. Given a community with S species, the exclusion ratio of species i, denoted as ER_i, is a relative metric that assesses whether the probability of exclusion for species i (P_i^E) is large by comparing it to that of an ideal symmetric community with the same number of species ($1/S$) (Equation 5). By definition, this metric ranges between 0 and infinity, and is equal to 1 only in symmetric communities. The larger the exclusion ratio of species i, the larger the relative probability that i can be the first species that is excluded.

Asymmetry index. This community-level metric describes the distribution of the average probabilities of exclusion $P_i^E(\mathbf{A}) \in [0, 1]$ and, thus, the (a)symmetry of the FD' shape. To quantify it, we use a commonly-used equitability index (sensu Tuomisto (2012)): the relative Shannon diversity index of the average probabilities of exclusion $P_i^E(\mathbf{A})$ (Equation 7).

occurs when the vector $\mathbf{r}$ is at the *incenter* of the FD $\mathfrak{I}$ (black plus markers in Figure 1) because its minimum distance to any edge of the FD is the same regardless of the direction of the perturbation (i.e isotropic perturbation). Thus, the maximum isotropic perturbation that a community can cope with, while being feasible, will be geometrically equivalent to the distance from the incenter to all the edges of the FD (along the surface of the unit ball), denoted by θ (dashed lines in Figure 1).

Now, we can ask how the shape of the FD influences the maximum perturbation of the incenter $\mathfrak{I}$. In general, when two communities follow Equation (1) and have the same number of species S and equal sizes of their FDs, the more asymmetric a FD is, the closer the edges are to the incenter $\mathfrak{I}$ and, consequently, the smaller the minimum distance between them θ (i.e. the smaller maximum perturbation). This difference is illustrated in our example for $S = 3$ species in Figure 1, where the maximum isotropic perturbation from the incenter is larger for the symmetric domain than for the asymmetric one ($\theta_{\text{symmetric}} = 0.417$ and $\theta_{\text{asymmetric}} = 0.365$, respectively). The calculations required to find the incenter $\mathfrak{I}$ and the maximum isotropic perturbation θ of a given interaction matrix $\mathbf{A}$ can be found in Suppl. Section 3. Nevertheless, comparing the FD of communities from empirical studies is not straightforward, as communities may vary both in species richness and in the degree of interaction asymmetry between species. This variation in the size and number of species will consequently affect the shape of the FD. The next sections are therefore dedicated to explaining under realistic conditions how changes in the shape of the FD allow us to understand and predict the magnitude of perturbations that species can withstand (exclusion distance) and the probability of exclusion for species and entire communities.

Feasibility domain shape: Species exclusion distances

In the previous section, to answer the question of which is the maximum random perturbation a community can handle without losing species, we considered the distance from a specific point, the incenter ($\mathfrak{I}$), to the edges of the FD (θ). However, the same question can be explored by taking any other initial vector of growth rates within the FD $\mathbf{r}_0 \neq \mathfrak{I}$. In this more general case, we can find the point in the border of the FD ($\mathbf{r}_{0,\text{min}}$) at a minimum distance to the initial vector of growth rates ($\mathbf{r}_0$). That distance between $\mathbf{r}_0$ and the closest point in the border $\mathbf{r}_{0,\text{min}}$, θ_0, defines the maximum perturbation that will cause one of the S species to be excluded. The advantage here is that the approach can further inform us about which species will go extinct first: the identity of such species only depends on the location of $\mathbf{r}_{0,\text{min}}$ on the border of the FD. Following the example in Figure 2a, the closest point to the initial vector of growth rates $\mathbf{r}_0$ (blue circle) that is located on the border of the FD is $\mathbf{r}_C \equiv \mathbf{r}_{0,\text{min}}$ (orange square), and it is on the edge where species C is excluded (orange edge).

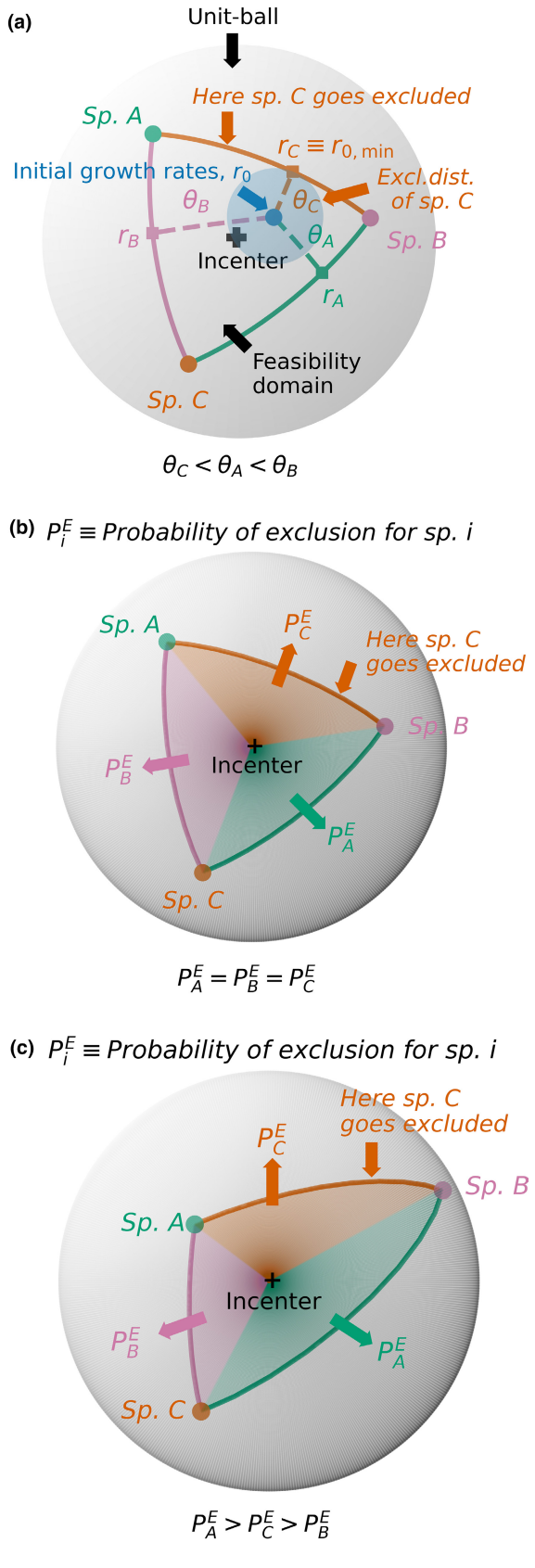

FIGURE 2 (a) Exclusion distances θ_i and maximum perturbation $\theta_0 (\equiv \theta_C)$ for the community in Figure 1a when the initial vector of growth rates $\mathbf{r}_0$ (dark blue dot) is not at the incenter (black plus marker). Dashed lines represent the exclusion distances (i.e. the shortest distances along the unit ball from the initial vector of growth rates (r_0) to the border where a given species goes extinct (square markers)). The colours of squares and dashed lines are those of the species excluded. The exclusion distances depicted in this example are $\theta_A = 0.407$, $\theta_B = 0.546$ and $\theta_C = 0.239$, respectively. (b) Representation of the average probabilities of exclusion for the species in the FD shown in Figure 1a: $P_A^E = P_B^E = P_C^E = 0.333$. The colours correspond to those of the species that will be the first ones to be excluded. (c) This panel shows the same information in Figure 2b for the FD in Figure 1b. In this asymmetric FD, the average probabilities of exclusion are $P_A^E = 0.444$, $P_B^E = 0.212$ and $P_C^E = 0.344$, respectively. The size of all the FDs included in this figure is the same ($\Omega = 0.064$).

In many situations, such as in conservation and restoration efforts, we are interested in the persistence of particular species, which poses the question of whether we can calculate such maximum perturbation before losing a given species i from the community. To do so, we simply need to calculate the minimum distance (along the unit ball) from $\mathbf{r}_0$ to the edge of the FD where i goes excluded, denoted by $\theta_{0,i}$. This distance is what we define as *species exclusion distances*. In Figure 2a, we represent the exclusion distances for the initial vector of growth rates $\mathbf{r}_0$ with dashed lines.

Feasibility domain shape: Probabilities of exclusion and exclusion ratios

In order to estimate the species exclusion distances θ_i we need quite a lot of information on the system, namely: the structure (matrix) of species interaction $\mathbf{A}$, which defines the FD, along with a vector of intrinsic growth rates, $\mathbf{r}_0$. However, characterizing such vector can be a challenging, labor-intensive work even in small communities (Bartomeus et al., 2021) and, hence, this information is not available for many communities, usually those including animal and long-lived species. In these cases, we can use the above definitions and a probabilistic perspective to estimate $P_i^E(\mathbf{A})$, the probability that species i will be the first one to be excluded if a strong perturbation took place:

$$P_i^E(\mathbf{A}) = \frac{\mathrm{vol}\left(r_0 \in \left(D_F(\mathbf{A}) \cap B^S\right) | \, \mathbf{r}_{0,\min} \in \varepsilon_i\right)}{\mathrm{vol}\left(D_F(\mathbf{A}) \cap B^S\right)}, \quad (4)$$

where ε_i represents the edge of the FD in which species i goes excluded. Note that this probability is formulated independently from the precise specification of initial conditions, similar to the structural forecasting in Saavedra et al. (2020). According to Equation (4), the probability $P_i^E(\mathbf{A})$ corresponds to the proportion of the FD's volume where the vectors of intrinsic growth rates are closer to the edge where species i is excluded (Figure 2). Therefore, by definition, $P_i^E(\mathbf{A}) < 1$ for $S > 1$ (when $\mathbf{A}$ is non-degenerate). We name the quantity $P_i^E(\mathbf{A})$ as the *probability of exclusion for species i*.

The probability of exclusion of a given species depends on the size and shape of the FD. As Figure 2

illustrates, such probabilities are mainly conditioned by the distance between the species vertices (circles) and the incenter (plus markers): the closer the vertex of a given species is to the incenter $\mathfrak{I}$ (compared to other vertices), the larger the probability that such species will be the first one to be excluded, and therefore the whole community will not be longer feasible. This prediction is important because it implicitly indicates that the shape of the FD can be characterized by computing the average probabilities of exclusion. For instance, in communities where all species interact in the same way, and consequently have symmetric FDs, all vertices are at the same distance from the incenter and the probability of exclusion is the same for all species $P_i^E(\mathbf{A}) = 1/S$ (see Figure 2b for an example). In contrast, the larger the variation across the probabilities of exclusion, the larger the asymmetry of the FD because species present also asymmetries in their interaction matrix (e.g. effect on species i on j is not the same as the effect on species j on i). Our approach allows to assess whether the probability of exclusion for a given species is larger compared to a situation in which all species interact in the same way and therefore are equally likely to be the first species excluded:

$$ER_i(\mathbf{A}) = \frac{P_i^E(\mathbf{A})}{1/S}. \tag{5}$$

We denote such quantity as the *species exclusion ratio* (García-Callejas et al., 2023) (see Suppl. Section 5 for a generalization of Equation (5)). If $ER_i(\mathbf{A}) < 1$ ($ER_i(\mathbf{A}) > 1$), then the probability of exclusion of species i is smaller (larger) than that of a symmetric community. So we hypothesize that the smaller the value of $ER_i(\mathbf{A})$, the larger the species probability of persistence.

Finally, to compute the average probabilities of exclusion $P_i^E(\mathbf{A})$ in Equation (4) and the exclusion ratios derived from them in Equation (5) and Equation (S9), we propose the following approach:

$$P_i^E(\mathbf{A}) = \frac{\Omega\left(\mathbf{A}_i^M\right)}{\Omega(\mathbf{A})}, \tag{6}$$

where $\mathbf{A}_i^M$ represents a modified interaction matrix, obtained by replacing the vertex of species i (V_i) by the incenter, $\mathfrak{I}$, which is equivalent to replace the i-th column of $\mathbf{A}$ by the negative of the incenter's column vector. Intuitively, the solid angle $\Omega\left(\mathbf{A}_i^M\right)$ is the proportion of the volume of the unit ball where the vectors of growth rates are closer to the edge where species i is excluded (i.e. $\mathbf{r}_{0,\min} \in \varepsilon_i$). If we consider the examples in Figure 2b,c, we simply say that the area occupied by a given colour (e.g. green) is equal to the area obtained when placing the green vertex of species A in the position of the incenter.

It is worth noting that using the same quasi-Monte Carlo method applied to estimate Equation (3), we can compute efficiently both the numerator and denominator in Equation (6), and the results obtained are in excellent agreement with those obtained by simulating the dynamics of the underlying LV model (Equation 1) (see Suppl. Section 6 for details on the LV simulations, as well as examples in communities with three and more species). This might seem a technical detail but it has important implications for the application of our metrics by a broad range of ecologists. The problem we solve here is that finding several initial conditions randomly for estimating $P_i^E(\mathbf{A})$ from numerical simulations is a time-intensive task when the size of the FD is small ($\Omega \lesssim 10^{-12}$) with orders of magnitude that vary from minutes-hours with our approach to days-weeks with the numerical LV estimation (Figure S7). On top of this problem, solving the LV model numerically can be far from trivial when the abundance of certain species grows indefinitely, as in communities with mutualistic interactions and weak self-regulation. For those reasons, the estimation of the average probabilities of exclusion $P_i^E(\mathbf{A})$ from Equation (6) (via quasi-Monte Carlo method) is—to the best of our knowledge—the most efficient alternative to computing species-level probabilities of exclusion from a structuralist point of view.

Feasibility domain' shape: Asymmetry index

Taking into account the features of the probabilities of exclusion ($P_i^E(\mathbf{A}) \in [0, 1]$) and their link with the shape of the FD, we use a relative Shannon diversity index J', introduced by Pielou (1976), to describe the distribution of the average probabilities of exclusion. This index, which in our context we called 'asymmetry index', is a commonly-used equitability index in ecological studies (Tuomisto, 2012). It has the following three desirable properties: (i) it is maximal and equal to one when the average probabilities of exclusion are equal (i.e when the FD is symmetric); (ii) it approaches zero when the average probabilities of exclusion are very dissimilar; and (iii) the index shows values in the middle of its scale when the differences between probabilities can be intuitively considered 'intermediate' (see a full description of its features in (Smith & Wilson, 1996)). The asymmetry index is of the form:

$$J'(\mathbf{A}) = \frac{-\sum_{i=1}^{S} P_i^E(\mathbf{A}) \log\left(P_i^E(\mathbf{A})\right)}{\log(S)}, \tag{7}$$

for a community with S species. We use the notation $J'(\mathbf{A})$ to highlight the dependence of the results on the interaction matrix. Since $P_i^E(\mathbf{A})$ depends on the size of the FD, the latter also affects $J'(\mathbf{A})$. Indeed, given FDs whose sides are proportional, the larger the size of a given domain, the greater the differences among $P_i^E(\mathbf{A})$ and, thus, the more asymmetric (i.e. the smaller $J'(\mathbf{A})$) (Figure S8 for

an example). Nevertheless, the dependence of $P_i^E(\mathbf{A})$ and $J'(\mathbf{A})$ on size is smaller than that of other shape indices. In particular, we tested the relative change in shape indices in situations in which the size of the FD changes while its shape is kept approximately constant (Suppl. Section 7 for details). We show that, for communities of different sizes, the asymmetry index $J'(\mathbf{A})$ is much less sensitive to variations in size than two other indices, namely the variance of the cosine of the side lengths as developed by Grilli et al. (2017), and the variance of the niche differences developed by Saavedra et al. (2017) (Figure 3).

APPLICATIONS TO EMPIRICAL COMMUNITIES

With the perspective presented above and the proposed structural metrics, we can advance our understanding of the feasibility, composition and short-term dynamics of ecological communities. Importantly, this approach is valid for interactions among species belonging to a single trophic level, that is, communities driven by competition and facilitation, as well as for communities with relevant interactions across trophic levels, such as food webs or bipartite networks. We provide in the following sections two complementary analyses of natural communities. First, we expand on the use of our approach to predict short-term population growth rates using data from a highly-resolved annual plant community. Second, in Box 2, we evaluate the extinction risk of plants and pollinators based on the structure of their bipartite interactions.

Predicting plant population dynamics

Our main prediction is that the asymmetry of species interactions, which can be computed with the above-described shape-based metrics, modulates the population dynamics of species and therefore, can inform of temporal changes in species abundances and population growth rates, at least in the short term. In addition, it can also inform on the expected variability of population growth rate across time. If these hypotheses hold, our approach can help predict changes in abundance in species-rich communities while maintaining a mechanistic understanding (Ehrlén & Morris, 2015). In particular, our first theoretical expectation is that, the smaller the exclusion ratio (ER_i) or the larger the exclusion distance (θ_i) of a given species, the larger the perturbation needed to exclude it from the community. Hence, it is more likely that these species will exhibit positive short-term growth rates because they will tend to increase their populations (Figure 4). Complementing this hypothesis, we also expect that those species with a smaller exclusion ratio (ER_i) will present higher variation in population

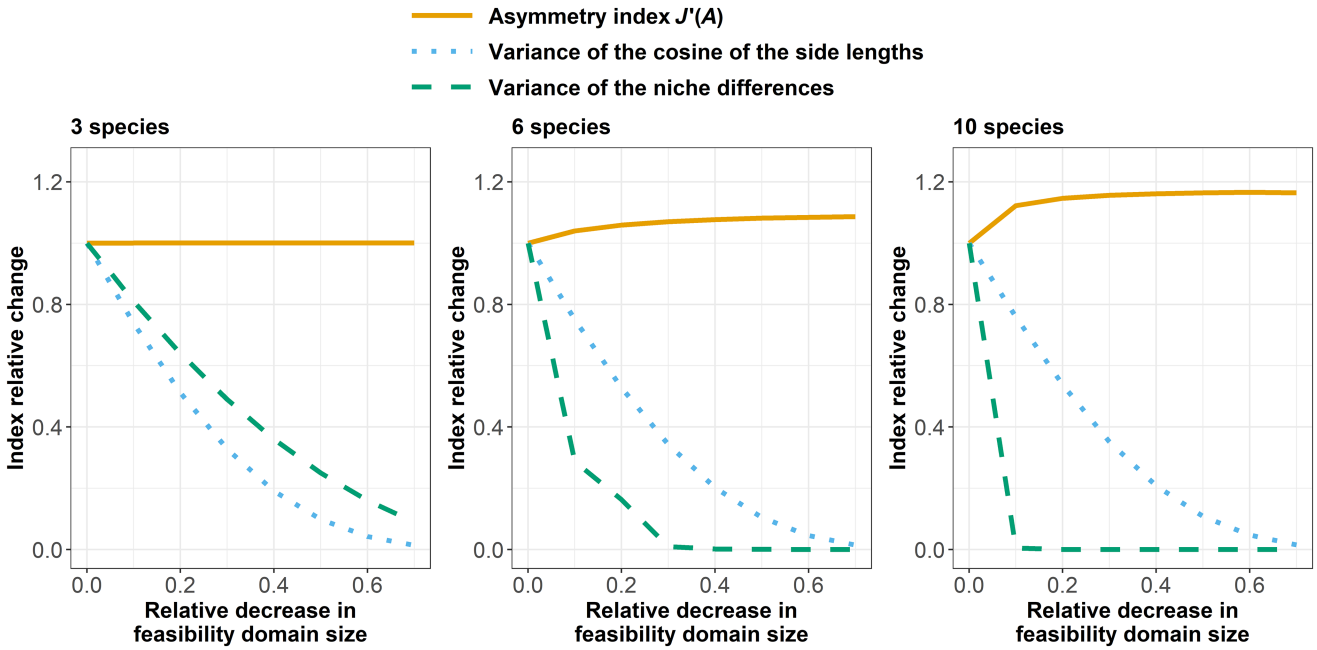

FIGURE 3 Dependence of several shape indices on the size of the feasibility domain (FD) and species richness. For 3, 6 and 10 species we show how much the value of the three indexes evaluated vary (y-axis) when we reduce the size of the FD but preserve the proportions of the distances between the domain's vertices (x axis). The indexes shown are: the asymmetry index $J'(\mathbf{A})$ (continuous lines), the variance of the cosine of the side lengths developed by Grilli et al. (2017) (dotted lines) and the variance of the niche differences developed by Saavedra et al. (2017) (dashed lines). A value of index relative change equal to one means that the index value is maintained across reductions of the FD. The metric we present in this perspective ('asymmetry index') slightly varies as we account for more species in the community but this variation is negligible compared to previous indices available in the literature. A graphic example of how the size of the FDs is reduced while maintaining the proportions among its sides is given in Suppl. Section 7.

growth rates, while this variation will be reduced in species with a larger exclusion ratio (ER_i) (Suppl. Section 8). This is because, for species presenting a small ER_i, the perturbation can occur in many different directions, either promoting or hindering population growth across time, but is less likely to occur in the specific direction that promotes the extinction of such species. Conversely, for a species presenting a large ER_i, any perturbation is more likely to head in the multiple directions that promote its exclusion, so in order to persist, such species with large ER_i will only withstand small perturbations. This implies small changes in population growth rates in the long term (Arnoldi et al., 2018). Finally, we predict that the more accurate the structural characterization of the community (by providing information on species interactions and their intrinsic growth rates), the better the prediction. That is, we expect that predictions based on detailed structural information, such as the exclusion distances θ_i (extracted from species' intrinsic growth rates at a given time), will perform better than those derived from a probabilistic average, like the exclusion ratios ER_i (Figure 4).

Empirical information to test our three central predictions comes from a detailed observational study in species-rich plant communities from a Mediterranean grassland. There, we gathered information on the observed abundances, intrinsic reproduction rates and interactions between annual plant species for 7 years, from 2015 to 2021 (García-Callejas et al., 2021).

Study system

From November 2014 to September 2021, we sampled each year at Caracoles Ranch, located in Doñana National Park, SW Spain (37°04′01.0″ N, 6°19′16.2″ W), 19 annual species naturally occurring in the study area, which accounted for > 90% of plant biomass in the community. These 19 species belong to disparate taxonomic families and exhibit contrasted functional profiles along the growing season (Supplementary Table S1). The earliest species with small size and open flowers, such as *Chamaemelum fuscatum* (Asteraceae), peak at the beginning of the growing season (February), while late species with succulent leaves, such as *Salsola soda* (Amaranthaceae), grow during summer and peak at the end of the growing season (September–October).

In order to parameterize empirical estimates of intra- and interspecific pairwise plant–plant interactions (i.e. the elements α_{ij} of the interaction matrices $\mathbf{A}$) we related species' individual reproductive success to the number of potentially competing individuals of each species within plant neighbourhoods for each year, which allow us to extract the seed production in the absence of neighbours λ, the growth vector $\mathbf{r}$ and $\mathbf{A}$ (see further details in García-Callejas et al. (2021), Lanuza et al. (2018) and in Suppl. Section 10). Aside from these data, we also recorded annually an independent measure of field abundance for

BOX 2 Assessing exclusion risks in mutualistic communities with shape-based metrics: A proof of concept

The structure of plant-pollinator interactions can encapsulate information about the sensitivity of different species to perturbations. For example, there is considerable evidence supporting the relationship between specialization and extinction risk (Bartomeus et al., 2013; Biella et al., 2020; Burkle et al., 2013; Memmott et al., 2007; Scheper et al., 2014): extinction risk declines with increasing numbers of mutualist partners, from least-linked (most specialized) species to most-linked (most generalized) ones.

Here, we test if the ranking of our shape-based metrics, which quantify the species' average probability of being the first species excluded from a given community, aligns with the expected relationship between specialization and extinction risk described in the literature. To do so, we extracted from the Mangal database (Poisot et al., 2016) 88 empirical plant-pollinator networks from five different studies with wide geographical coverage (Table S14). Such data comprises 1734 species in total, where 1198 species were animals. On average each network had 19.70 ± 9.18 nodes of which 13.61 ± 6.94 were animals. For each of these networks, we estimated the communities' effective interaction matrices using the mean field approximation for intra-guild competition and the two inter-guild parameterizations proposed in (Saavedra, Rohr, Olesen, et al., 2016) for mutualistic communities. Then, we extracted the species' probability of exclusion, $P_i^E(\mathbf{A})$ using Equation (6). We quantified probabilities of exclusion instead of exclusion distances because we lack estimations of intrinsic growth rates in these 88 communities.

Results using the shape-based metrics show that the probability of exclusion $P_i^E(\mathbf{A})$ is moderately but significantly correlated with species degree ($r = -0.37$, $\text{C.I.}(95\%) = [-0.395, -0.338]$, $p\text{-value} < 2 \cdot 10^{-12}$) when analysing the 88 networks together. Interestingly, our analysis identified that on average pollinators are at more immediate risk of exclusion than plants, although the trend is not statistically significant due to the large variability across individual networks ($P^E_{\text{pollinators}}(\mathbf{A}) = 0.054 \pm 0.028$, $P^E_{\text{plants}}(\mathbf{A}) = 0.044 \pm 0.035$). These results are in line with previous empirical and theoretical findings (Biella et al., 2020; Memmott et al., 2004). Our results were robust when considering alternative mean-field interactions among species (Suppl. Figures S21 and S22), and are encouraging considering the potential biases and differences in sampling methodologies across networks.

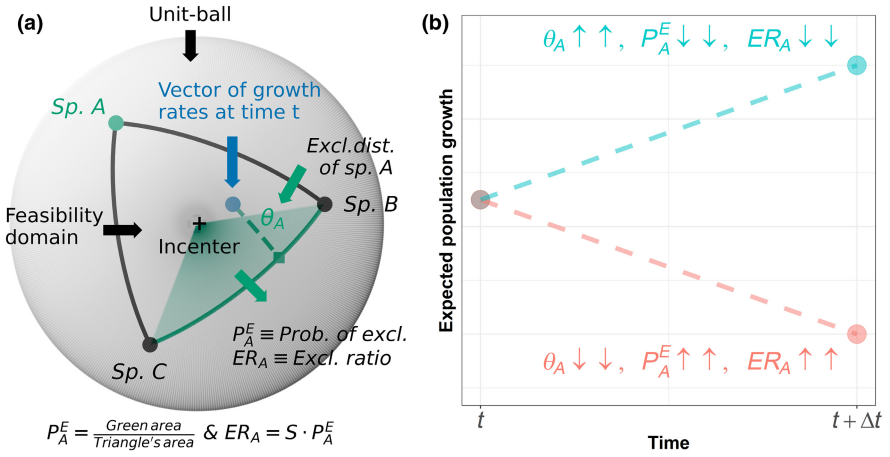

FIGURE 4 (a) Example of the shape-based exclusion metrics that can be estimated for a species that belongs to a (symmetric) community with $S = 3$ species, namely: the exclusion distance of species A (θ_A), its probability of exclusion (P_A^E) and its corresponding exclusion ratio (ER_A). (b) Expected relationships between the shape-based exclusion metrics of a single species in a given year (t) and its future population growth ($t + \Delta t$).

each of the 19 species considered (Suppl. Table S1). The sampling coverage of plant–plant interactions, quantified via rarefaction curves, was > 99% in all annual communities (Suppl. Section 12).

Estimation of shape-based metrics

Using the empirical estimates of the interaction matrices and intrinsic growth rates, we obtained the annual exclusion distances and the exclusion ratios for the 19 plant species in our system. The former was derived from Equation (S7), whereas the latter was estimated from Equations (3) and (5), via quasi-Monte Carlo methods based on Equation (6), generating 10,000 random draws for each required value of exclusion probability, $P_i^E(\mathbf{A})$. For these calculations, we assumed that the interaction coefficients and the exclusion metrics represent the corresponding averaged values within a given year, while these average values vary across years due mainly to inter-annual variation in rainfall. In addition to the structural metrics, we tested whether the interaction matrices of our system were diagonal-stable (Suppl. Section 11). Our analyses showed no evidence of diagonal stability. Hence, we cannot ensure that dynamical stability is fulfilled in addition to feasibility. This apparent contradiction does not affect the following analyses, because we explored year-to-year changes in population growth rate and its relationship with exclusion metrics based on interannual realizations of the interaction matrix. Although long-term dynamical stability might not be relevant for our understanding of the short-term dynamics of annual plant communities in which their biotic interactions are reset each hydrological year, it is important to bear in mind that proving such dynamical stability is a necessary condition for predicting which species will persist at long-term equilibrium (Saavedra et al., 2017).

Statistical analyses

We analysed the relationship between the observed annual growth rate in our grassland study system, defined as $N_{i,t+1}/N_{i,t}$, and two of our metrics: the species exclusion ratio ER_i (based only on the interaction structure) and the species exclusion distance θ_i (based on both the interaction structure and the demographic performance). Note that abundance data are completely independent of the data used to calculate the interaction strengths (see details in García-Callejas et al. (2021)). Therefore, they provide a rigorous test to evaluate the ability of our metrics to predict the population dynamics of interacting species.

We developed two sets of regression models to test the relationship of annual population growth rate with our metrics. For the first set of six models, we implemented generalized linear models with Gamma and Gaussian distributions with log-link function, and took as single explanatory variables, respectively, the number of individuals of species i in the previous year, and two shape metrics of species i from the community in the previous year: the exclusion ratio $ER_i(\mathbf{A}_t)$ and the exclusion distance $\theta_i(\mathbf{A}_t)$. The second set of models is conceptually similar, but we fitted a negative exponential relationship (Non-lineal least squares [NLS] fit), in practice using $\log_{10}(N_{i,t+1}/N_{i,t}+1)$ as the response variable, following visual observations of the scatter-plot. We further tested for the inclusion of temporal autocorrelation structure that allows for unequally spaced time observations (CorAR1 in R-package nlme v3.1-152 Pinheiro et al. (2021)), as well as species identity as a random effect. Then, we compared those models on the basis of AIC to asses which model better described the patterns observed (Burnham & Anderson, 2004). For these analyses, given that not all the estimated interaction matrices contained the same pool of plant species, we only used the results for those species that were present from 2015 to 2021. In addition, we did not consider the data of the growing season of 2018 (that is, we did not try to predict the population growth in 2018 from the data in 2017) because that growing season was dominated by an extreme flooding event, which does not reflect the annual plant dynamics (see García-Callejas et al. (2021) for details on that perturbation and its effects on the community).

By applying the above filtering, we selected seven plant species from contrasted taxonomic groups, namely: *Beta macrocarpa*, *Centaurium tenuiflorum*, *Hordeum marinum*, *Leontodon maroccanus*, *Parapholis incurva*, *Polypogon maritimus* and *Salsola soda*.

Overall, in these models, we assumed that the relevant abiotic and biotic factors that drove the species dynamics during a given year were encoded in our shape-based metrics (Ehrlén & Morris, 2015). In addition, note that our models did not include information on the dispersal ability of the focal species, but given the nature of the study system which flooded every year, we assume there is no limitation to global dispersal in the study area.

Our analyses were conducted in R, with the `stats` v4.1.0 (R Core Team, 2021) and `lme4` v1.1-28 (Bates et al., 2015) packages. We also checked model assumptions with the R-package `nlstools` v2.0-0 (Baty et al., 2015).

RESULTS

In our 7 years of sampling, we documented and parameterized 126 and 2142 intra- and interspecific pairwise plant–plant interactions, respectively. From them, we extracted seven different annual interaction matrices **A**, whose average number of species per year was 15.29 ± 3.35. The estimated interaction strengths α_{ij} (the elements of **A**) were either negative (i.e. denoting competition) or positive (i.e. denoting facilitation). Further, the distribution of the absolute value of α_{ij} was right-skewed throughout all the years, with a majority of comparatively weak interactions (Suppl. Figure S11). The variation of those asymmetries in interaction strengths, as expected, also exerted changes in the size and shape of the communities' FD. This result is consistent with the idea that species sensitivity to perturbations is dependent on the system state and its structure of interactions with other species, as in the case of food webs (Beauchesne et al., 2021) or systems out-of-equilibrium (Medeiros et al., 2023). The maximum values of FD size (Ω) and symmetry (J') were reached from 2016 to 2018 ($\Omega_{max} = 0.382$ and $J'_{max} = 0.940$), and the minimum ones in 2019 and 2020 ($\Omega_{min} = 0.0823$ and $J'_{max} = 0.478$) being 0.5 and 1 the upper bounds of Ω and J' (Suppl. Figure S12). In general, the vulnerability to exclusion of the seven species present every sampled year, expressed via their exclusion ratios and exclusion distances, fluctuates across years (Suppl. Figures S13–S15).

Results from our models supported our theoretical expectations that our shaped-based metrics allow describing short-term population growth dynamics and their variance across time. Models that included shape metrics provided a better fit than the model only including abundance from the previous year, suggesting that the metrics considered carry a predictive signal. In particular, a NLS fit better described the observed relationships, as confirmed by comparing AIC values of the different models (Table S13). Therefore, we subsequently present the results obtained from the exponential NLS fits. These models show that the higher the exclusion ratio, the lower the growth rate of the following year (effect size: −0.31, Table S9). That is, those species that have larger probabilities of exclusion reduced their population growth rate the following year. Conversely, the exclusion distances have a positive effect on the population growth rate (effect size: 3.33, Table S12) indicating that those species that were further away from the edge of the FD increased their population growth rate the following year. We hypothesized that metrics with more detailed structural information would be better predictors of population growth rate, that is, models including exclusion distances would provide better fits than models based on exclusion ratios or raw probabilities of exclusion. This was not the case, as models incorporating different metrics showed similar AIC values, within a range of 63.862 ± 0.6192 units (Table S13). Here, we, therefore, focus on the model with exclusion ratio as the predictor, which showed the lowest AIC values and allows for a clear ecological interpretation (Figure 5). In that model, analysing the observed and predicted population growth allows a qualitative categorization of the observations in three groups. Those years in which species presented an exclusion ratio between 0 and 0.75 showed positive population growth rates on average and a greater variance, as predicted by our second hypothesis and supported by our simulations (Suppl. Figure S10). Conversely, we observed flat or negative population growth rates as well as the lower variance for species that showed an exclusion ratio > 0.75 in a certain year, particularly if the exclusion ratio was > 1.25. This suggests that, in our system, an exclusion ratio of 0.75 qualitatively differentiates species showing contrasted population growth trends across time. Lastly, accounting for species as random intercepts or for temporal autocorrelation did not improve model fits.

DISCUSSION

A central theme in ecology is which information we need to mechanistically understand and predict the vulnerability of species to perturbations coming, for example, from environmental changes. This question can be approached from different angles: from looking at physiological tolerances to different environmental stressors to analysing species' demographic vital rates, or to exploring the joint response of species interacting with each other. In this perspective, we show that adopting a community context, supported by a reliable quantification of species interactions, is critical to predicting the effect of environmental perturbations on the persistence of both particular species and entire communities. The

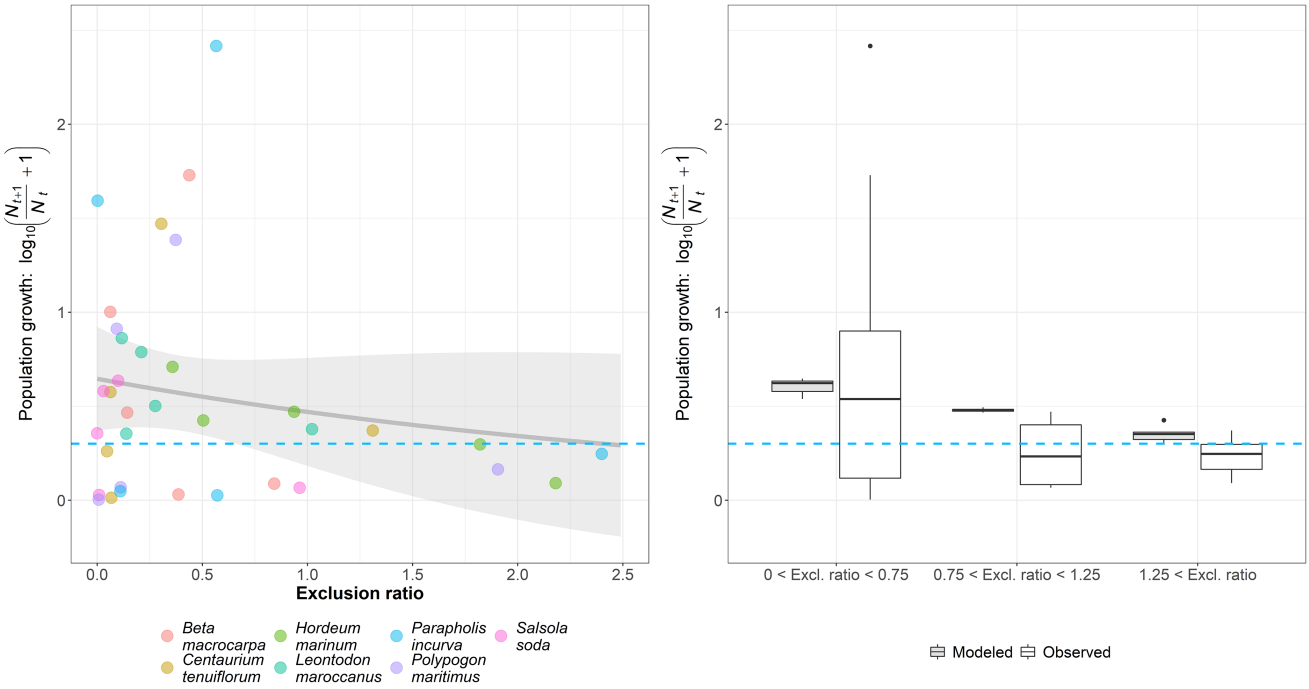

FIGURE 5 Results for the non-linear model $\log_{10}(\text{Pop. growth} + 1) = a \cdot \exp(b \cdot \text{Excl. ratio})$, showing the effect of the exclusion ratio in a given year t on observed population growth rate $N_{i,t+1} / N_{i,t}$. The left panel shows the observed values of exclusion ratio and population growth for each studied plant species (coloured dots), and the values predicted by the NLS model (grey line), and their 95% confidence interval (grey shaded area). Above the blue dashed line population growth increases $(N_{i,t+1} > N_{i,t})$, whereas below that line it decreases $(N_{i,t+1} < N_{i,t})$. Box plots in the right panel display the observed and predicted population growth across three different groups of exclusion ratios: (i) $ER_i < 0.75$, (ii) $0.75 < ER_i < 1.25$ and (iii) $1.25 < ER_i$.

joint possibility of keeping a mechanistic understanding of how biodiversity is maintained across ecological levels of organization (individual species and entire communities) while achieving a reasonable predictive power is now possible by acknowledging the idea that species present in natural systems show asymmetries in their biotic interactions, and, therefore, the size and the shape of the community feasibility domain should be simultaneously explored.

A remarkable finding is that the shape-based metrics developed here are useful to predict changes in year-to-year effective growth rates among interacting species in a grassland system (see Table S13). This is a strong result taking into account that the studied species are annual plants whose abundances depend on a myriad of biotic and abiotic factors including variation in precipitation, dispersion and natural enemies (Petry et al., 2018). Overall, these results suggest that, although simplistic, the structure of species interactions and species' demographic performance phenomenologically capture key ingredients of the processes controlling population dynamics and are more meaningful for making predictions that just considering abundances from previous years. Interestingly, our results suggest that experimentally deriving intrinsic growth rates, a difficult parameter to estimate empirically (Bartomeus et al., 2021), might not be critical to obtaining reliable predictions. Further work can build on this framework to, for example, study not only the probability of exclusion but its *velocity* (Medeiros et al., 2021).

Overall, these results reinforce the idea that increasing system complexity is not incompatible with the predictability of the dynamics of its components (Daugaard et al., 2022). Rather, our results emphasize that the interaction structure of the system, which varies from year to year, implying concomitant variations in the size and shape of the FD, is in itself ecologically relevant for predicting short-term demographic performance. As shown in Box 2, this framework can accommodate more complex communities considering not only plants but also several trophic levels, such as plant-pollinator systems or multi-trophic communities (García-Callejas et al., 2023). Empirically documenting all relevant competitive, mutualistic and trophic interactions of a community is the next step needed to percolate the use of theoretically-informed tools to better understand and predict the temporal dynamics of ecological systems.

The metrics we propose here integrating species-level sensitivity to perturbations (i.e. the range of reproductive outcomes that lead to species persistence) within a community-level measure of feasibility (i.e. the *asymmetry index*) do not start from scratch. They rather build on previous efforts (Grilli et al., 2017; Medeiros et al., 2021; Saavedra et al., 2017; Tabi et al., 2020) that identified a key issue in the structuralist approach: the size of the FD, by itself, is not fully representative of the capacity of a

community to withstand perturbations. Rather, we need to quantify its shape, i.e. the relative contribution of each species to it. Both properties are not fully independent in spherical geometry, which is the mathematical backbone of the structuralist approach (Suppl. Section 2). However, just like we might expect for two proportional triangles in two-dimensional geometry to have the same 'shape' according to a quantifiable metric, we might approach that intuitive requirement in spherical geometry. Our asymmetry index fulfils this requirement more robustly than previous approaches, i.e. it's much less sensitive to variations in the size of the FD for a given shape (Figure 3). We provide implementations of all the metrics discussed here in the R package `anisoFun` v1.0: https://github.com/RadicalCommEcol/anisoFun, and we suggest that their adoption may help bridge the gap between ecological theory and empirical studies, in order to provide robust quantitative solutions to manage, conserve and restore biodiversity. For instance, highly asymmetric FDs due to high asymmetries in biotic interactions among species are indicative of strong differences in species probabilities of exclusion. This first-order analysis can be used as an indicator, in applied contexts, that detailed analyses of extinction risk are necessary. On the contrary, such additional risk analyses would not be so critical to perform in symmetric FDs, where all species have a similar probability of exclusion.

Both feasibility and dynamic stability are necessary conditions for the long-term coexistence of species at equilibrium (Bunin, 2017; Takeuchi, 1996). We did not find evidence of diagonal stability in the interaction matrices of our study system, implying that although the communities are mathematically feasible, they are likely to be unstable in the long term, that is, external perturbations to species abundances would drive the system out of equilibrium. This notion, however, applies to long-term equilibrium analyses, which are not the main scope of our study. Rather, we are interested in short-term, year-to-year predictions of the system. In particular, our metrics can be useful in (1) predicting short-term population growths (left panel in Figure 5) and (2) understanding its expected variability (right panel in Figure 5). Our results show that species with high exclusion ratios have lower variability in their population growth rate across years (Suppl. Section 8), which may indicate slower recovery rates from perturbations (Arnoldi et al., 2018). Nevertheless, it is important to bear in mind that the exclusion distances, probabilities of exclusion and exclusion ratios discussed here are asymptotic properties of the system, and thus remain approximations of the underlying dynamics of complex ecological communities.

The applicability of these metrics for a wide range of systems and community types remains an open question, but we can anticipate some limitations. On the theoretical side, we assume that the basic elements contained in the structure of species interactions (i.e. pairwise interactions) vary across years but can be well-approximated by annually-averaged values within a given year and that functional forms (i.e. the relationship between species abundances and overall interaction effects) are linear. However, the existence of non-linear functional forms for modelling pairwise interactions (or even the addition of higher order interactions as in Gibbs et al. (2022)) will have non-trivial consequences on system dynamics (Dougoud et al., 2018) and may preclude the use of the linear definition of the FD that sustains our approach. This framework is, nevertheless, able to accommodate different types of interactions beyond plant–plant interactions (Box 2), as well as alternative functional forms and dynamics (such as those of the saturating competition model by Brauer and Castillo-Chavez (2011) and other examples in Cenci and Saavedra (2018) and Saavedra et al. (2017)). On the empirical side, it is premature to generalize these results to other systems because the importance of obtaining robust demographic performance data and the predictive skill gained with it is likely to be context-dependent. For instance, a single demographic performance value might not be as meaningful for systems with more complex life cycles. Overall, we argue that the toolbox developed here is ready to be used for systems whose species display similar population dynamics and similar responses to external perturbations (e.g. annual plant communities, coral reef fishes, tropical trees, plant-pollinator mutualistic systems) (Box 2; García-Callejas et al., 2023).

CONCLUSION

Reliable tools for predicting ecological outcomes remain elusive and, in general, disconnected from those frameworks used to understand ecological processes. Here, we provide a novel set of metrics within a structuralist approach that considers the conditions leading to the persistence of species and entire ecological systems. This stems from the fact that biotic interactions among species are asymmetric in their strength and sign within ecological communities. Our overall aim with this perspective is to advance in advancing our mechanistic understanding of the maintenance of biodiversity in ecological communities while simultaneously increasing the predictive ability of their dynamics. We have shown that including information on species interactions and their demographic performance in the estimation of these shape-based structural metrics significantly improves short-term predictions of species abundances in an annual plant community, compared to predictions based only on species' previous abundances. The species and community-level metrics presented here are general across interaction types and can be efficiently obtained for ecological communities of arbitrary richness, unlocking the possibility of systematically studying the biotic control over ecological dynamics for a wide range of levels of diversity and organisms.

AUTHOR CONTRIBUTIONS

Alfonso Allen-Perkins, David García-Callejas and Oscar Godoy designed the study. David García-Callejas, Oscar Godoy and Ignasi Bartomeus collected data. Alfonso Allen-Perkins and David García-Callejas developed the shape-based metrics. Alfonso Allen-Perkins, David García-Callejas and Oscar Godoy designed the analyses and Alfonso Allen-Perkins implemented them. All authors wrote the first draft of the manuscript and contributed substantially with revisions.

ACKNOWLEDGEMENTS

We thank the Radical Community Ecology group (https://github.com/RadicalCommEcol/) for the fruitful discussions. AA-P, DGC, IB and OG were funded by the Spanish Ministry of Science and Innovation (MICINN) and the European Social fund through the MeDiNaS (RTI2018-098888-A-I00), TASTE (PID2021-127607OB-I00) and ChaSisCOMA (PID2021-122711NB-C21) projects. Additionally, OG acknowledges financial support provided by the Spanish Ministry of Economy and Competitiveness (MINECO) and by the European Social Fund through the Ramón y Cajal Program (RYC2017-23666).

PEER REVIEW

The peer review history for this article is available at https://www.webofscience.com/api/gateway/wos/peer-review/10.1111/ele.14291.

DATA AVAILABILITY STATEMENT

The data and code used to generate the results of this study are available at https://doi.org/10.5281/zenodo.8087366 and https://github.com/RadicalCommEcol/Asymmetric_Interactions. The `anisoFun` package v1.0 is available at https://github.com/RadicalCommEcol/anisoFun and https://doi.org/10.5281/zenodo.8086505.

ORCID

Alfonso Allen-Perkins https://orcid.org/0000-0003-3547-2190
David García-Callejas https://orcid.org/0000-0001-6982-476X
Ignasi Bartomeus https://orcid.org/0000-0001-7893-4389
Oscar Godoy https://orcid.org/0000-0003-4988-6626

REFERENCES

Adler, P.B., Smull, D., Beard, K.H., Choi, R.T., Furniss, T., Kulmatiski, A. et al. (2018) Competition and coexistence in plant communities: intraspecific competition is stronger than interspecific competition. *Ecology Letters*, 21, 1319–1329.

Arnoldi, J.-F., Bideault, A., Loreau, M. & Haegeman, B. (2018) How ecosystems recover from pulse perturbations: a theory of short-to long-term responses. *Journal of Theoretical Biology*, 100, 79–92.

Barabás, G.J., Michalska-Smith, M. & Allesina, S. (2016) The effect of intra-and interspecific competition on coexistence in multispecies communities. *The American Naturalist*, 188, E1–E12.

Bartomeus, I., Park, M.G., Gibbs, J., Danforth, B.N., Lakso, A.N. & Winfree, R. (2013) Biodiversity ensures plant-pollinator phenological synchrony against climate change. *Ecology Letters*, 16, 1331–1338.

Bartomeus, I., Saavedra, S., Rohr, R.P. & Godoy, O. (2021) Experimental evidence of the importance of multitrophic structure for species persistence. *Proceedings of the National Academy of Sciences of the United States of America*, 118, e2023872118.

Bascompte, J., Jordano, P. & Olesen, J.M. (2006) Asymmetric coevolutionary networks facilitate biodiversity maintenance. *Science*, 312, 431–433.

Bates, D., Machler, M., Bolker, B. & Walker, S. (2015) Fitting linear mixed-effects models using lme4. *Journal of Statistical Software*, 67, 1–48.

Baty, F., Ritz, C., Charles, S., Brutsche, M., Flandrois, J.-P. & Delignette-Muller, M.-L. (2015) A toolbox for nonlinear regression in R: the package nlstools. *Journal of Statistical Software*, 66, 1–21.

Beauchesne, D., Cazelles, K., Archambault, P., Dee, L.E. & Gravel, D. (2021) On the sensitivity of food webs to multiple stressors. *Ecology Letters*, 24, 2219–2237.

Biella, P., Akter, A., Ollerton, J., Nielsen, A. & Klecka, J. (2020) An empirical attack tolerance test alters the structure and species richness of plant-pollinator networks. *Functional Ecology*, 34, 2246–2258.

Bimler, M.D., Stouffer, D.B., Lai, H.R. & Mayfield, M.M. (2018) Accurate predictions of coexistence in natural systems require the inclusion of facilitative interactions and environmental dependency. *Journal of Ecology*, 106, 1839–1852.

Brauer, F. & Castillo-Chavez, C. (2011) *Mathematical models in population biology and epidemiology. Texts in applied mathematics*, 2nd edition. New York, NY: Springer.

Bunin, G. (2017) Ecological communities with lotka-volterra dynamics. *Physical Review E*, 95, 042414.

Burkle, L.A., Marlin, J.C. & Knight, T.M. (2013) Plant-pollinator interactions over 120 years: loss of species, co-occurrence, and function. *Science*, 339, 1611–1615.

Burnham, K.P. & Anderson, D.R. (2004) Multimodel inference. *Sociological Methods & Research*, 33, 261–304.

Cenci, S. & Saavedra, S. (2018) Structural stability of nonlinear population dynamics. *Physical Review E*, 97, 012401.

Cenci, S., Song, C. & Saavedra, S. (2018) Rethinking the importance of the structure of ecological networks under an environment-dependent framework. *Ecology and Evolution*, 8, 6852–6859.

Civantos-Gómez, I., García-Algarra, J., García-Callejas, D., Galeano, J., Godoy, O. & Bartomeus, I. (2021) Fine scale prediction of ecological community composition using a two-step sequential machine learning ensemble. *PLoS Computational Biology*, 17, e1008906.

Clark, A.T., Ann Turnbull, L., Tredennick, A., Allan, E., Harpole, W.S., Mayfield, M.M. et al. (2020) Predicting species abundances in a grassland biodiversity experiment: trade-offs between model complexity and generality. *Journal of Ecology*, 108, 774–787.

Daugaard, U., Munch, S.B., Inauen, D., Pennekamp, F. & Petchey, O.L. (2022) Forecasting in the face of ecological complexity: number and strength of species interactions determine forecast skill in ecological communities. *Ecology Letters*, 25, 1974–1985.

Dietze, M.C. (2017) Prediction in ecology: a first-principles framework. *Ecological Applications*, 27, 2048–2060.

Dougoud, M., Vinckenbosch, L., Rohr, R.P., Bersier, L.-F. & Mazza, C. (2018) The feasibility of equilibria in large ecosystems: a primary but neglected concept in the complexity-stability debate. *PLoS Computational Biology*, 14, e1005988.

Ehrlén, J. & Morris, W.F. (2015) Predicting changes in the distribution and abundance of species under environmental change. *Ecology Letters*, 18, 303–314.

Evans, J.S., Murphy, M.A., Holden, Z.A. & Cushman, S.A. (2011) Modeling species distribution and change using random forest. In: Drew, C., Wiersma, Y. & Huettmann, F. (Eds.) *Predictive species and habitat modeling in landscape ecology*. New York: Springer, pp. 139–159.

García-Callejas, D., Bartomeus, I. & Godoy, O. (2021) The spatial configuration of biotic interactions shapes coexistence-area relationships in an annual plant community. *Nature Communications*, 12, 6192.

García-Callejas, D., Godoy, O., Buche, L., Hurtado, M., Lanuza, J.B., Allen-Perkins, A. et al. (2023) Non-random interactions within and across guilds shape the potential to coexist in multi-trophic ecological communities. *Ecology Letters*, 26, 831–842.

Genz, A. & Bretz, F. (2009) *Computation of multivariate normal and t probabilities*. Lecture notes in statistics, 2009th edition. Berlin, Germany: Springer.

Gibbs, T., Levin, S.A. & Levine, J.M. (2022) Coexistence in diverse communities with higherorder interactions. *Proceedings of the National Academy of Sciences of the United States of America*, 119, e2205063119.

Godoy, O., Bartomeus, I., Rohr, R.P. & Saavedra, S. (2018) Towards the integration of niche and network theories. *Trends in Ecology & Evolution*, 33, 287–300.

Godoy, O. & Levine, J.M. (2014) Phenology effects on invasion success: insights from coupling field experiments to coexistence theory. *Ecology*, 95, 726–736.

Gourion, D. & Seeger, A. (2010) Deterministic and stochastic methods for computing volumetric moduli of convex cones. *Computational and Applied Mathematics*, 29, 215–246.

Grilli, J., Adorisio, M., Suweis, S., Barabas, G., Banavar, J.R., Allesina, S. et al. (2017) Feasibility and coexistence of large ecological communities. *Nature Communications*, 8, 14389.

Hart, S.P., Freckleton, R.P. & Levine, J.M. (2018) How to quantify competitive ability. *Journal of Ecology*, 106, 1902–1909.

Lanuza, J.B., Bartomeus, I. & Godoy, O. (2018) Opposing effects of floral visitors and soil conditions on the determinants of competitive outcomes maintain species diversity in heterogeneous landscapes. *Ecology Letters*, 21, 865–874.

Lepori, V.J., Loeuille, N. & Rohr, R.P. (2023) Robustness vs productivity during evolutionary community assembly: short-term synergies and long-term trade-offs. *bioRxiv*, 2022.10.14.512255.

Levine, J.M., Bascompte, J., Adler, P.B. & Allesina, S. (2017) Beyond pairwise mechanisms of species coexistence in complex communities. *Nature*, 546, 56–64.

Logofet, D.O. (2005) Stronger-than-Lyapunov notions of matrix stability, or how "flowers" help solve problems in mathematical ecology. *Linear Algebra and its Applications*, 398, 75–100.

Macarthur, R.H. (1957) On the relative abundance of bird species. *Proceedings of the National Academy of Sciences of the United States of America*, 43, 293–295.

McGill, B.J., Etienne, R.S., Gray, J.S., Alonso, D., Anderson, M.J., Benecha, H.K. et al. (2007) Species abundance distributions: moving beyond single prediction theories to integration within an ecological framework. *Ecology Letters*, 10, 995–1015.

Medeiros, L.P., Allesina, S., Dakos, V., Sugihara, G. & Saavedra, S. (2023) Ranking species based on sensitivity to perturbations under non-equilibrium community dynamics. *Ecology Letters*, 26, 170–183.

Medeiros, L.P., Song, C. & Saavedra, S. (2021) Merging dynamical and structural indicators to measure resilience in multispecies systems. *Journal of Animal Ecology*, 90, 2027–2040.

Memmott, J., Craze, P.G., Waser, N.M. & Price, M.V. (2007) Global warming and the disruption of plant-pollinator interactions. *Ecology Letters*, 10, 710–717.

Memmott, J., Waser, N.M. & Price, M.V. (2004) Tolerance of pollination networks to species extinctions. *Proceedings of the Royal Society B: Biological Sciences*, 271, 2605–2611.

Peñuelas, J., Canadell, J.G. & Ogaya, R. (2011) Increased water-use efficiency during the 20th century did not translate into enhanced tree growth. *Global Ecology and Biogeography*, 20, 597–608.

Petchey, O.L., Pontarp, M., Massie, T.M., Kefi, S., Ozgul, A., Weilenmann, M. et al. (2015) The ecological forecast horizon, and examples of its uses and determinants. *Ecology Letters*, 18, 597–611.

Petry, W.K., Kandlikar, G.S., Kraft, N.J., Godoy, O. & Levine, J.M. (2018) A competition-defence trade-off both promotes and weakens coexistence in an annual plant community. *Journal of Ecology*, 106, 1806–1818.

Pielou, E.C. (1976) *Ecological diversity*. Nashville, TN: John Wiley & Sons.

Pinheiro, J., Bates, D., DebRoy, S., Sarkar, D. & R Core Team. (2021) *nlme: linear and nonlinear mixed effects models*. R package version 3.1-152. Available at: https://CRAN.R-project.org/package=nlme [Accessed 28th June 2023].

Poisot, T., Baiser, B., Dunne, J.A., Kéfi, S., Massol, F., Mouquet, N. et al. (2016) Mangal—making ecological network analysis simple. *Ecography*, 39, 384–390.

R Core Team. (2021) *R: a language and environment for statistical computing*. Vienna, Austria: R Foundation for Statistical Computing. Available from: https://www.R-project.org/

Saavedra, S., Medeiros, L.P. & AlAdwani, M. (2020) Structural forecasting of species persistence under changing environments. *Ecology Letters*, 23, 1511–1521.

Saavedra, S., Rohr, R.P., Bascompte, J., Godoy, O., Kraft, N.J. & Levine, J.M. (2017) A structural approach for understanding multispecies coexistence. *Ecological Monographs*, 87, 470–486.

Saavedra, S., Rohr, R.P., Fortuna, M.A., Selva, N. & Bascompte, J. (2016) Seasonal species interactions minimize the impact of species turnover on the likelihood of community persistence. *Ecology*, 97, 865–873.

Saavedra, S., Rohr, R.P., Olesen, J.M. & Bascompte, J. (2016) Nested species interactions promote feasibility over stability during the assembly of a pollinator community. *Ecology and Evolution*, 6, 997–1007.

Scheper, J., Reemer, M., van Kats, R., Ozinga, W.A., van der Linden, G.T.J., Schaminée, J.H.J. et al. (2014) Museum specimens reveal loss of pollen host plants as key factor driving wild bee decline in The Netherlands. *Proceedings of the National Academy of Sciences of the United States of America*, 111, 17552–17557.

Shoemaker, L.G., Sullivan, L.L., Donohue, I., Cabral, J.S., Williams, R.J., Mayfield, M.M. et al. (2019) Integrating the underlying structure of stochasticity into community ecology. *Ecology*, 101, e02922.

Smith, B. & Wilson, J.B. (1996) A consumer's guide to evenness indices. *Oikos*, 76, 70–82.

Song, C., Rohr, R.P. & Saavedra, S. (2018) A guideline to study the feasibility domain of multi-trophic and changing ecological communities. *Journal of Theoretical Biology*, 450, 30–36.

Song, C. & Saavedra, S. (2018) Structural stability as a consistent predictor of phonological events. *Proceedings of the Royal Society B: Biological Sciences*, 285, 20180767.

Song, C., Von Ahn, S., Rohr, R.P. & Saavedra, S. (2020) Towards a probabilistic understanding about the context-dependency of species interactions. *Trends in Ecology & Evolution*, 35, 384–396.

Tabi, A., Pennekamp, F., Altermatt, F., Alther, R., Fronhofer, E.A., Horgan, K. et al. (2020) Species multidimensional effects explain idiosyncratic responses of communities to environmental change. *Nature Ecology and Evolution*, 4, 1036–1043.

Takeuchi, Y. (1996) *Global dynamical properties of Lotka-Volterra systems*. Singapore: World Scientific.

Tredennick, A.T., Hooker, G., Ellner, S.P. & Adler, P.B. (2021) A practical guide to selecting models for exploration, inference, and prediction in ecology. *Ecology*, 102, e03336.

Tredennick, A.T., Hooten, M.B. & Adler, P.B. (2017) Do we need demographic data to forecast plant population dynamics? *Methods in Ecology and Evolution*, 8, 541–551.

Tuomisto, H. (2012) An updated consumer's guide to evenness and related indices. *Oikos*, 121, 1203–1218.

Venturelli, O.S., Carr, A.C., Fisher, G., Hsu, R.H., Lau, R., Bowen, B.P. et al. (2018) Deciphering microbial interactions in synthetic human gut microbiome communities. *Molecular Systems Biology*, 14, e8157.

SUPPORTING INFORMATION

Additional supporting information can be found online in the Supporting Information section at the end of this article.

How to cite this article: Allen-Perkins, A., García-Callejas, D., Bartomeus, I. & Godoy, O. (2023) Structural asymmetry in biotic interactions as a tool to understand and predict ecological persistence. *Ecology Letters*, 26, 1647–1662. Available from: https://doi.org/10.1111/ele.14291